SINGLE SHOT BUNCH-BY-BUNCH BEAM EMITTANCE MEASUREMENT OF THE SPRING-8 LINAC

Yoshihiko Shoji[#] and Kouji Takeda, NewSUBARU/SPring-8, University of Hyogo, Japan

Abstract

The bunch-by-bunch emittance of a single shot beam from the SPring-8 electron linac was measured utilizing phase rotation in an electron storage ring. The linac beam was injected into the ring and the beam profiles of several revolutions were recorded using a dual sweep streak camera. The fast sweep separated the linac bunches in 1 ns macro pulse and the slow sweep separated the profiles at different turns. The bunch emittances were reconstructed from the profiles. The stability of the linac beam was evaluated from the recorded shot-to-shot fluctuation. We also identified differences in the orbit and the emittance of different bunches in a pulse.

INTRODUCTION

The SPring-8 linac has been operated as an injector to the electron storage ring, NewSUBARU. However, fine parameter tuning is required for stable top-up injection because of the small ring acceptance. In that process, single shot linac beam monitors were necessary to understand the shot-to-shot fluctuation of the injection. A single shot bunch-by-bunch emittance monitor would be a powerful tool to understand the shot-to-shot fluctuation of the injection efficiency.

We used the visible light profile monitor of the electron storage ring as a diagnostic for the linac beam. The dual sweep streak camera recorded multiple profiles of the injected beam in a single camera frame. The fast sweep separated linac bunches in a macro pulse and the slow sweep separated profiles of different turns. The betatron oscillation in the ring produced phase rotation allowing the reconstruction of the beam emittance. It was possible to fully optimize the ring parameters for our measurements since beam storage was not required.

A stability of the linac beam was evaluated from the shot-to-shot variation. We could also see differences in the bunch at the front of a macro pulse compared to the bunch at the rear.

PARAMETERS OF DAILY OPERATION

Averaged Beam Parameters

Figure 1 shows the layout of the SPring-8 linac, the booster synchrotron, and NewSUBARU storage ring. Table 1 shows the main parameters for the linac. The macro pulse width of the linac beam is normally 1 ns, which contains 3 linac bunches. The rf synchronization system between the linac and the ring [1] enables an injection to a single rf bucket of the ring with rf frequency of 500 MHz.

_____
[#] shoji@lasti.u-hyogo.ac.jp

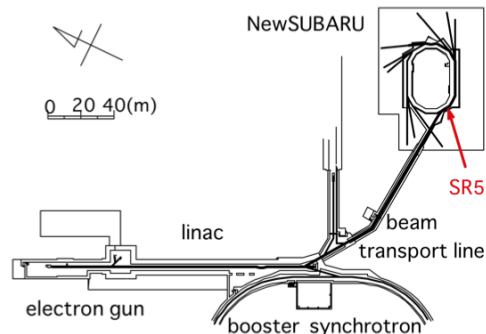Figure 1: Layout of the 1 GeV SPring-8 linac, the booster synchrotron, and the NewSUBARU storage ring.

Table 1: Main Parameters of the Linac

Electron energy	1 GeV
Rf frequency	2856 MHz
Common pulse rate	1 Hz
Common pulse width	1 ns
FWHM bunch length; front/middle	10 ps / 14ps
Full energy spread; front / middle	0.4% / 0.6%
Transverse emittance (FWHM^2)	100 π nmrad.

The listed transverse emittance was calculated from the average over many shots, measured by Q-scanning at the beam transport line. The longitudinal parameters were obtained from the measurements of the synchrotron oscillation in the ring just after injection [2]. The listed bunch length and the energy spread were calculated from the average of 10 shots.

Bunch Structure and Injection Efficiency

The bunch structure was fluctuated by a jittering of the gate pulse of the electron gun. Figure 2 shows six typical dual sweep images of the streak camera with six typical bunch structures. The vertical axis in the images is the ring rf phase and the horizontal axis the revolution. The time structure at 1/4 of the synchrotron oscillation period (41 μs) gives the energy profile.

Figure 3 shows the injection efficiency with the ring parameters characteristic of daily operation. Shots with images A and B had comparatively worse efficiency. A separated data shows that the ring has a large enough longitudinal acceptance for the injected beam, suggesting that dependence on transverse parameters caused fluctuations in the injection efficiency.
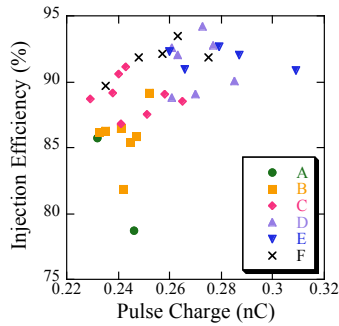
Figure 3: Injection efficiency for different bunch structure.

Figure 2: Typical dual sweep images.

SHOT-TO-SHOT MEASUREMENTS

Setup for the Measurement

Figure 4 shows the schematic layout near the injection point and the monitor line, named SR5. The dove prism on the line switches transverse measurement axis, in this case we selected the vertical with 90 degrees rotation.
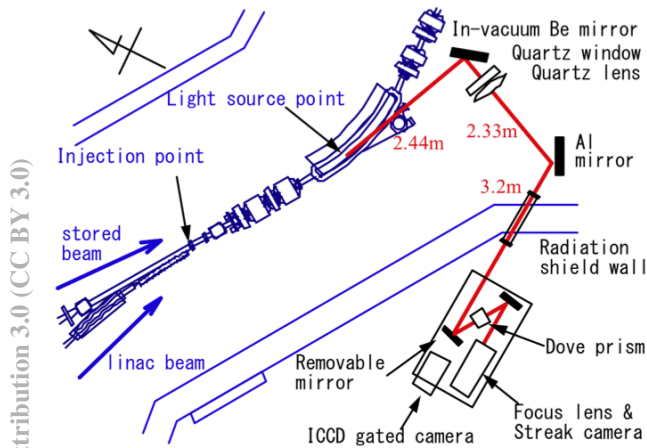

Figure 4: Layout of the visible light monitor line SR5.

The ring parameters were different from those of daily operation. The injection pulse bump was optimized so that the injected beam had a small dipole oscillation and maintained almost 100% injection efficiency. The vertical chromaticity was reduced to 0 in order to eliminate the betatron phase spread over multiple revolutions. The linear H/V coupling was reduced to less than 1%. The very small beam size of the stored beam was used to calibrate the vertical spatial resolution: 0.3 mm FWHM at the light source point with $\beta_y = 17$ m.

Data Analysis of a Typical Shot

Here we demonstrate our method of analysis using a representative shot (#12) as an example. Its total charge, measured by fast CT on the beam transport line, was 0.23 nC.

Figure 5 shows the dual sweep image of the streak camera frame and the projection to the fast sweep axis. The vertical axis is the horizontal position in space and the ring rf phase in time. The upper part of the figure corresponds to the head of the linac pulse with the tail in
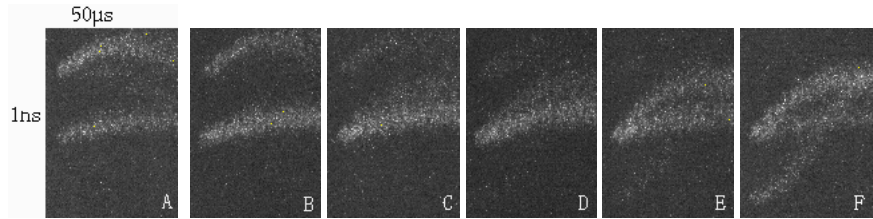
the lower part of the figure. The horizontal axis is the vertical position in space and the ring revolutions in time. The six spots correspnd to profiles from the 4th through 9th turns after the injection. Profiles at the initial 3 turns were out of the camera slit because of a large horizontal displacement. The horizontal profile in the figure of each spot corresponds to the vertical spatial profile in the experimental frame.

Figure 6 shows profiles of the 6 turns of the two respective bunches. They were fitted with Gaussian functions. We derived the peak position y and a divergence σ^2 as a function of the revolution number N.
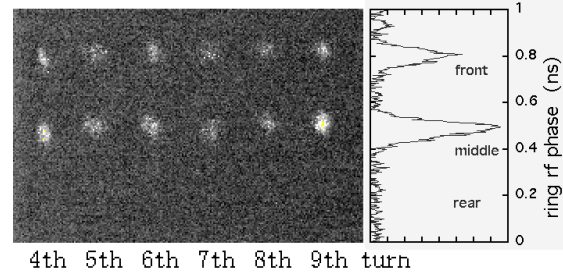

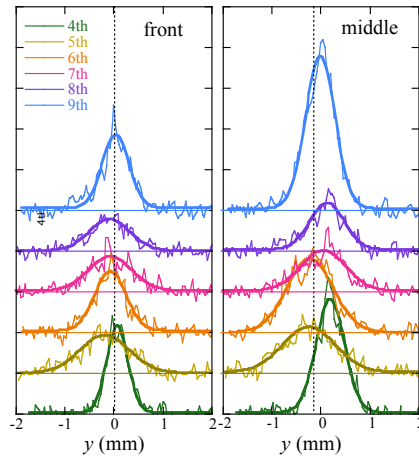Figure 5: Dual Sweep image of the injected beam of the shot #12.

Figure 6: Vertical beam profiles from turns 4 through 9 of the front bunch and the middle bunch.

As shown in Figure 7, the data were fitted with the following sinusoidal functions

$$y = A_0 + A_S \sin(2\pi\Delta\nu_y N) + A_C \cos(2\pi\Delta\nu_y N) \qquad (1)$$

$$\sigma^2 = B_0 + B_S \sin(4\pi\Delta\nu_y N) + B_C \cos(4\pi\Delta\nu_y N) \qquad (2)$$

Here $\Delta\nu_y = 0.224$ is the sub-integer part of the vertical betatron tune. The dipole oscillations of two bunches were obviously different. The oscillations of the widths

were almost the same except for one data point, the 6th turn of the middle bunch.

The beam ellipse at the injection point is calculated using the phase advance to the light source point, 0.15 rad. Figure 8 shows the extrapolation of the fitted wave and the beam ellipses at the injection point.

The transverse emittance ε_y was obtained from

$$\varepsilon_y = \sqrt{(B_0 - \sigma_R^2)^2 - (B_S^2 + B_C^2)}\,/\beta_y. \qquad (3)$$

Here $\sigma_R^2 = 0.02$ mm^2 is the spatial resolution.
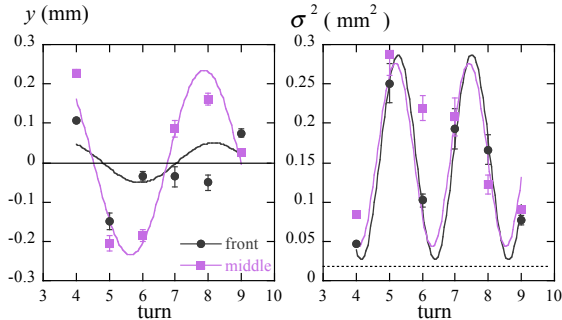
Figure 7: The dipole oscillation of the peak position (left) and the quadrupole oscillation of the divergence (right). The dotted line on the right indicates the spatial resolution.
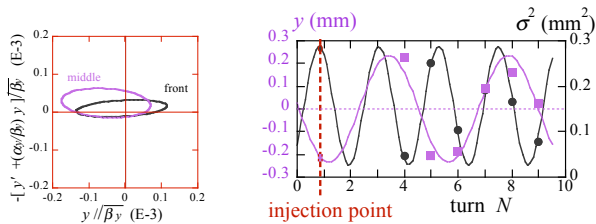

Figure 8: Extrapolation of the fitted waves and the calculated beam ellipses at the injection point.

Shot-to-Shot Fluctuation

We recorded the profiles of 20 shots in order to see the shot-to-shot fluctuation. Figure 9 shows the bunch charge for the 20 shots. They are grouped A-E, according to the charge of the front bunch.
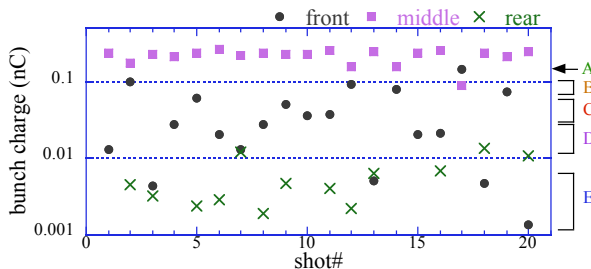

Figure 9: Bunch charge for the highlighted 20 shots.

The parameters quantifying the dipole oscillation, A_C and A_S, of the middle bunch are plotted in Figure 10. The fluctuation was correlated with the group and took place at the phase $\Delta A_S / \Delta A_C = 1.3$. We added data points of the front bunch of groups A–C to the plot. The differences in the same pulse were roughly of the order of the fluctuation in phase.

The parameters for the quadrupole oscillation, B_C and B_S, of the middle bunch are plotted in Figure 11. No clear dependence on the group was observed. However, it seems to be no accident that the difference of two bunches satisfied $2\Delta B_S - \Delta B_C > 0$ for all 8 shots.
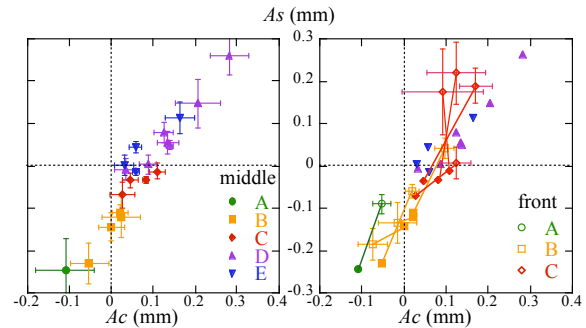

Figure 10: Shot-to-shot fluctuation of the dipole oscillation of the middle bunch (left) and those of the front bunch (right). The oscillations of different bunches in the same shot are connected with lines.
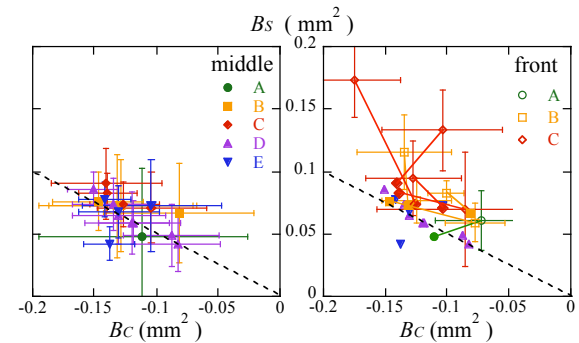

Figure 11: Shot-to-shot fluctuation of the quadrupole oscillation of the middle bunch (left) and those of the front bunch (right).

SUMMARY AND DISCUSSION

We succeeded in measuring the shot-to-shot, bunch-by-bunch fluctuations of the vertical emittance of the SPring-8 linac beam. A measurement of the horizontal parameter would be necessary to identify the mechanism that causes the correlation with the injection efficiency.

ACKNOWKEDGEMENT

REFERENENCES

[1] Y. Kawashima, *et al.*, PR ST-AB 4, 082001 (2001).

[2] T. Matsubara, *et al.*, PR ST-AB 9, 042801 (2006).